INVESTIGATIONS INTO THE USE OF SHAPE MEMORY ALLOY FOR THE DESIGN OF OSCILLATORY PROPULSION SYSTEM

Nagahiko Shinjo[*] and Geoffrey W. Swain[†]
Ocean Engineering Program
Department of Marine and Environmental Systems.
Florida Institute of Technology
150 West University Blvd., Melbourne, FL 32901, USA.
*shinjon@fit.edu, †swain@fit.edu

Abstract

This study investigates the potential of incorporating the elastic mechanisms found fish muscles into mechanical systems for the development of underwater propulsion. Physical and kinematic information associated with the steady swimming of the bonito and other scombrid species was used for material selection and design. Several electroactive materials were examined for simulating muscle behavior and their relative suitability was compared. Dynamic analysis, such as a work-loop technique, provided information for material comparison and performance evaluation. Lack of dynamic information made any direct comparison between the biological and mechanical systems difficult. Based on available information, it was found that shape memory alloy (SMA) was best suited to produce relatively slow and powerful steady swimming motion. The geometry of tendon and muscular systems were adapted. These arrangements alleviate the limited strain of the SMA by trading force for distance and provide effective force transmission pathways to the backbone.

Introduction

Increasing demand for higher efficiency in order to achieve longer missions in autonomous underwater vehicles has led to a search for alternative propulsive mechanisms based on biological systems (Sfakiotakis et al., 1999). This is an effective way of developing innovative technological solutions since evolutionary processes have already performed the design iterations and the cost-benefit-analysis to optimize particular designs for specific functions (Fish and Rohr, 1998). Several mechanical prototypes have been built to exploit the potential benefits of fish-like oscillating propulsion (Ayers et al., 2000; Bandyopadhay, 1998; Triantafyllou and Triantafyllou, 1995). At present, hydrodynamic aspects of swimming mechanisms such as drag reduction and vortex control are the primary focus. However, internal components may also contribute to the power output and efficiency (Alexander, 1988). Until recently, such mechanisms have been overlooked from most design considerations. This paper reviews the swimming muscular systems and the synthetic materials that are available to provide muscle-like actions. The steady swimming of the bonito species was selected as the base model and shape memory alloy (SMA) was identified as the best candidate material to generate oscillatory mechanisms.

The ability of terrestrial animals as well as insects to conserve metabolic energy by using elastic stain energy during their locomotion is well documented (Alexander, 1988; Farley et al., 1993; Full, 1997; Nachtigall, 1974). Several studies have indicated as much as 50% of metabolic energy savings can be achieved in some terrestrial animals (Alexander, 1984; Biewener, 1998). Tendons are generally used as the elastic energy storage in large terrestrial animals (Alexander, 1988) while small terrestrial and aquatic animals have adapted muscles for the same effect (Biewener, 1998; Lindstedt et al., 2002; Westneat and Wainwright, 2001). The effective use of soft muscle tissues as energy storage requires elaborate activation schemes. So-called 'eccentric contraction' or 'active stretching' allows the dynamic changes in apparent muscle stiffness to store extra mechanical energy. This technique has considerable effect on muscle power output and efficiency in aquatic animals (Biewener, 1998).

Work-loop techniques have been adapted to examine the dynamic nature of active stretching (Josephson, 1985). The analysis provides the work and power outputs of muscle with various cyclic frequency, strain, and stimulation timing. This information is valuable for the design and evaluation of a mechanical counterpart, however such analysis has

rarely been performed on mechanical devices (Full and Meijer, 2000).

The present study examined the ability of electro-active materials to simulate muscle behavior. The following sections present general overviews of muscle properties, a dynamic analysis method, electroactive material properties, and a conceptual propulsion system design.

General muscle properties

The primary function of skeletal muscle is to generate a contractile force (McMahon, 1984). This relatively simple mechanism is found throughout the animal kingdom with very little change during evolution (White, 1977). Physical and mechanical properties of skeletal muscles are available from various sources (Carlson and Wilkie, 1974; McMahon, 1984; Nordin and Frankel, 2001).

Muscles are generally composed of basic contractile units called sarcomere; a long chain of sarcomere forms a myofibril and several bundles of myofibrils form a bulk muscle. Sarcomere contain contractile proteins called actin and myosin which appear in the form of thin and thick filaments respectively due to the partial overlapping of the filaments. Stimulations from a motor neuron initiate the interaction between the filaments via cross-bridges. Cross-bridges pull the thin filament in a ratchet-like manner to slide the thin filaments, resulting in the shortening of the sarcomere.

Most muscle fibers are activated in an 'all or nothing' manner; there is no partial activation but either fully active or completely inactive. Muscles respond to a stimulus from a motor neuron in two different ways; twitch and tetanus. A twitch is a muscle response given by a single stimulus and the action consists of a brief contraction followed by relaxation. Application of multiple stimuli before the effect of the previous stimulus has died away results in a summation effect. This repetitive stimulation is called tetanus and it generates a higher tensile force than the twitch action.

Source of elastic energy

The ability of elastic materials to store external sources of energy as elastic strain energy and release it as useful mechanical energy benefits the energy conservation in oscillatory mechanisms. A pogo stick analogy has been used to explain the benefit of this elastic effect during locomotion (Alexander, 1988). The cyclic motions of the locomotor (i.e. legs and body) involve constant changes in the energy flux in and out of the system. Deceleration requires the dissipation of energy which is generally wasted in the form of heat. Elastic materials harness this energy and release it in the subsequent motion, as supplemental energy, reducing energy input from the source.

Tendons are generally considered as the elastic energy storage in large terrestrial animals (Alexander, 1988). The relatively high modulus of a mammalian tendon (1.5 GPa at 2.2 Hz) has an energy recovery efficiency of about 93% (Ker, 1981). Ground traction and gravitational forces further enhance the elastic effects.

Tendons in swimming animals as well as small terrestrial animals are not proportioned to optimize the elastic effect (Altringham and Shadwick, 2001; Biewener, 1998; Lindstedt et al., 2002). Their primary function is to transmit force. Theoretical investigation on the effects of passive elastic materials in swimming animals did not provide sufficient evidence for the adaptation of tendons as energy storage (Bennett et al., 1987; Blickhan and Cheng, 1994). However some studies have indicated that storage and recovery of elastic strain energy can occur in the absence of tendons and that muscles can effectively be used as elastic energy storage (Lindstedt et al., 2002). The effective use of muscles as elastic energy storage requires proper muscle stimulation timings with respect to its strain cycles. The timing to enhance energy storing capability of muscles is called 'active stretching' or 'eccentric contraction' which involves initiating contraction while the muscle is lengthening. This condition increases the apparent stiffness of muscles and allows them to absorb extra mechanical work (Lindstedt et al., 2002). *In-vivo* muscle studies in several fish species have indicated that the timing and duration of muscle activation relative to the strain cycle can have considerable effects on both muscle power output and efficiency (Biewener, 1998; Lindstedt et al., 2002).

Dynamic muscle properties (work loop analysis)

Oscillatory movements of the locomotors, such as limbs and bodies, require muscles to develop force dynamically in a time-dependent manner to generate thrust against the surrounding fluid medium (Biewener, 1998). Quasi-static data on force-velocity and force-length relationships overlook realistic loading conditions and may not describe the muscle performance during locomotion (Josephson, 1985; Rome, 1994). Josephson (1985) adapted work

loop analysis for evaluating the dynamic performance of muscle fibers.

The idea is to strain muscles mechanically in a sinusoidal manner and obtain a corresponding force production cycle. The work output per cycle can be determined by plotting the force output against the strain cycle (Figure 1). The amount of work done by the muscle, or positive work, is represented in a counterclockwise loop while work done to the muscle, or negative work, is represented by a clockwise loop. The mechanical power output can be obtained by multiplying the work out put by the cycle frequency.

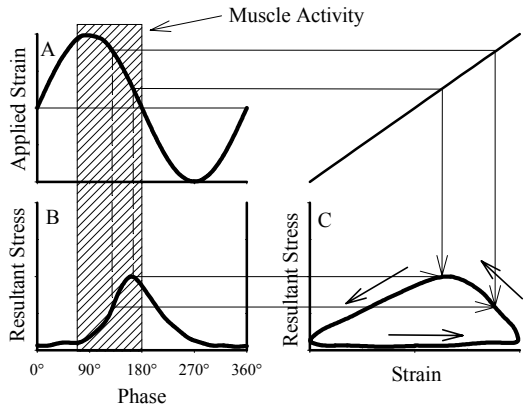

Figure 1. Schematic presentation work loop technique adapted from *(Josephson, 1985)*. A: strain cycles, B: force production. C: work-loop.

Figure 1A shows a cyclic length change of a muscle as a function of time and the corresponding muscle activities. The cyclic duration (x-axis) is generally subdivided into angular quantities. The y-axis represents the relative length change (strain). The maximum displacement occurs at 90º and 270º, which corresponds to the maximum extension and contraction respectively. Muscle shortening starts from 90º to 270º and lengthening occurs from 270º to 90º.

Figure 1B and C represent hypothetical force output and a corresponding work-loop plot. In general, large positive net work is produced when the peak force lags behind the strain cycle. Or contrarily, large negative net work is produced when the peak force leads the peak strain.

Work loop analysis has also been applied to measure in-vivo activity of muscles. Miniaturized sensing devices such as a sonomicrometry (an acoustic distance sensor) and piezoelectric crystal (a force sensor) can be inserted into the muscle, in order to monitor the muscle activity. An electromyogram (EMG) can also be incorporated to monitor electrical activity of the muscle.

Fish propulsive mechanisms

Swimming motion is generated by activating alternate sides of segmented muscles in a sequential manner. An anterior muscle is activated first and a wave of activation propagates from head to tail producing a backward traveling wave of body bending. The generation of the bending wave is determined by the following factors (Altringham and Shadwick, 2001)

- The muscle properties and activity patterns.
- The arrangement and the properties of passive elements in the body.
- The interaction between the fish and reactive forces of the water.

The locomotor musculatures in fish are arranged in a segmental manner and each segment or myomere forms a complex three-dimensional structure. The general shape of a myomere is shown in the following figure and detailed descriptions are also well documented (Alexander, 1969; Altringham and Ellerby, 1999; Nursall, 1956; Van Leeuwen, 1999; Westneat and Wainwright, 2001).

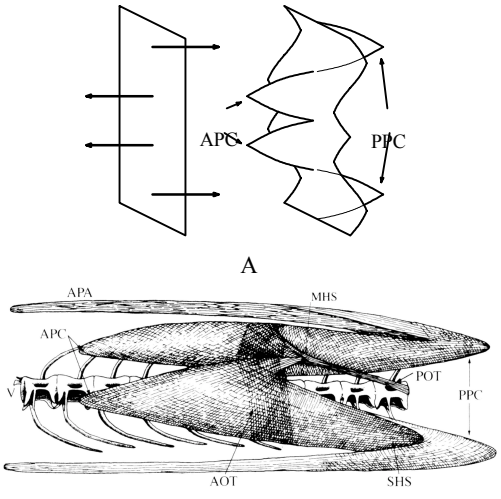

Figure 2. Myomere geometry. A. Schematic formation of myomere, B, Myomere drawing from *(Westneat and Wainwright, 2001)*. APC: anterior pointing cone, PPT: posterior pointing cone, AOT: anterior oblique tendon, POT posterior oblique tendon.

The shape of myomere resembles stretching of an elastic sheet (Figure 2A); two forward pointing

apexes at the mid section (anterior pointing cone, APC) and backward pointing apexes at the top and bottom (posterior pointing cone, PPC).

A myomere is composed of two distinct types of muscles; oxidative red and glycolic white muscles. The superficial red muscles are generally located along the mid lateral line just under the skin in a wedge formation. Several scombrid fish such as tuna and bonito possess internally located red muscles along the horizontal septum (Westneat and Wainwright, 2001). Red muscles are mainly used for long duration and low intensity activities such as steady swimming. The remaining muscle volume is occupied by white muscles which are used for short bursts of high intensity activities such as sprinting and escape maneuvers. The following Table depicts the red muscle properties of scombrid species.

Table 1: Scombrid Red muscle properties (Syme and Shadwick, 2002; Westneat and Wainwright, 2001)

Density	1050 kg/m^3
Relative red muscle mass	4-13%
Force output per unit area	140–174 kN/m^2
Power density	12–40W/kg
Work output per cycle	12-20 J/kg

Connective tissues

The locomotion of scombrid species depends critically on the transmission of force from muscles to the backbone via connective tissues, including the myosepta, the horizontal and vertical septa and the skin (Ellerby et al., 2000; Knower et al., 1999; Shadwick et al., 1999; Van Leeuwen, 1999; Wainwright, 1983; Westneat and Wainwright, 2001). Myoseptum is a connective tissue which separates two adjacent myomeres and transmit the force to the vertebra and skin. It is composed of two groups of collagen fibers running in different directions as can be seen in Figure 2B. One group of fibers are oriented longitudinally to form a posterior oblique tendon (POT) while the other group of fibers run vertically and wrap around the bases of the APC to from an anterior oblique tendon (AOT). Horizontal septa are attached to the backbone and extend towards the skin and are formed by the convergence of myosepta between the APC. The vertical septa form over the neural and hemal spines and hold the spines in position. The general force transfer mechanism from the superficial muscle to the backbone is illustrated in the following figure.

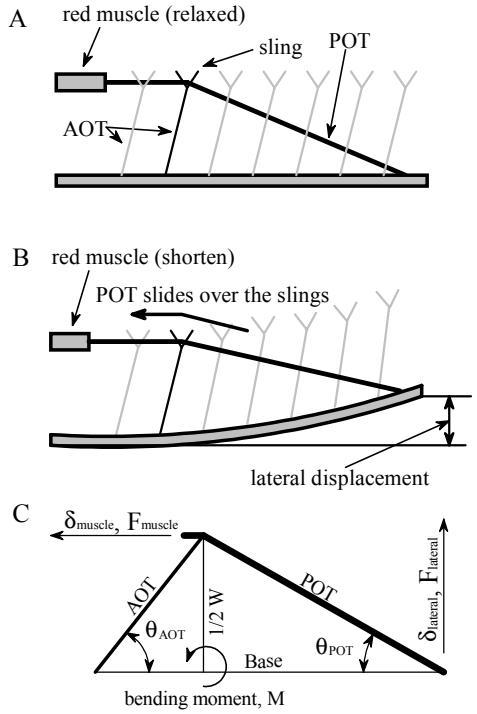

Figure 3. Bending mechanisms of scombrid fish adapted from *(Westneat and Wainwright, 2001)*. A. tendon arrangement, B. bending mechanism, C. schematic representation of the system

The POT length and the lateral distance from the backbone to the POT sling determine the amount of vertebra bending moment. An increase in lateral distance (W) or POT angle (θ_{POT}) will result in an increase in moment and a corresponding decrease in lateral displacement (δ_{displ}). The following Table shows the AOT and POT angles in scombrid species.

Table 2: AOT and POT angles with respect to the backbone in tuna and bonito species *(Westneat and Wainwright, 2001)*

Angle	Anterior	Posterior
AOT-backbone	50º	80º-90º
POT-backbone	40º	10º-15º

Steady Swimming kinematics

Red muscles power steady swimming of fish. The activation patterns of the muscle vary with body form and swimming mode but are independent of swimming speed (Altringham and Shadwick, 2001). The illustrations of EMG patterns for various species can be found in several references (Altringham and Johnston, 1990; Altringham and Shadwick, 2001; Ellerby et al., 2000; Knower et al., 1999; Shadwick et al., 1999).

Comparison between EMG activity and muscle strain cycle indicates the adaptation by fish of active stretching (refer to Figure 1A). The onset of EMG activities precedes the onset of muscle shortening by 30°-50° (Altringham and Shadwick, 2001; Ellerby et al., 2000; Shadwick et al., 1999). EMG activities cease late in the shortening phase at the anterior and cease early at the posterior sections indicating larger positive work production at the anterior sections. The following table shows the steady swimming kinematics in bonito (*Sarda Chiliensis*) and these parameters were used for the basis of the system design.

Table 3:Steady swimming kinematics of Bonito (Sarda Chiliensis) *(Ellerby et al., 2000)*

Swimming velocity		0.9-2.5BL	
Tail beat amplitude		0.19-0.21BL	
Tail beat frequency		1.2-3.2 Hz	
Stride length		0.75-0.77BL	
Mechanical wave length		1.07-1.13BL	
Mechanical wave propagation		1.34FL/T	
EMG activity propagation relative to strain cycle		1.66 FL/T	
Superficial red muscle strain	Anterior (0.35FL)	Middle (0.5 FL)	Posterior (0.65FL)
	±3.1%	±5.2%	±5.8%
EMG onset	52.9°	45.9°	36.8°
EMG offset	209.7°	180.2°	159.5°

Artificial muscle materials

Recent advancements in electroactive materials have shown the potential of actuators for emulating biological muscles. The actuation mechanisms of these materials occur at a molecular level which yields noiseless motion, miniaturization, and other advantages over conventional actuators. The elimination of gears, bearings, and other components reduce the mechanical complexity, size, and weight (Breazeal and Bar-Cohen, 2003). The flexible nature of many materials allows them to form almost any conceivable shape (Meijer et al., 2003). Active material based swimming vehicles have been used in several previous studies (Ayers et al., 2000; Shahinpoor et al., 1998; Webb et al., 2000).

In this study, electroactive polymer (EAP) and shape memory alloy (SMA) were considered for the actuator material. The physical and mechanical comparisons among these materials including mammalian muscles are available (Fletcher, 1996; Hollerbach et al., 1992; Kornbluh et al., 1998). The following sections briefly describe basic actuation mechanisms and the mechanical properties of the materials.

Shape Memory Alloy (SMA)

SMAs exhibit the ability to return to a predetermined shape upon application of heat (Hodgson, 1988; Jackson et al., 1972). They are a thermally driven actuator, however, the relatively high resistivity of the material allows electrical current to heat the material for shape changes. The reversible changes in crystalline structure or phase transformation are responsible for the memory effect; soft and ductile martensite structures at low temperature transform into strong and predetermined austenite structures at high temperature.

During the shape recovery, the material produces a recovery stress of approximately 200 MPa which is one of the highest among active materials. The phase transformation occurs in a simple shearing motion of the atoms within the crystal structure. Since no diffusion or large movement of atoms is required, the transformation occurs as fast as heat energy can be put into or taken out of the material. However the heat dissipation, by conduction and convection, is generally a slow process and this limits the operational frequency to about 1 Hz. The strain limit of the material is approximately 5-8%.

Electroactive polymer (EAP)

The elastic nature of many EAPs allow integration of elasticity into a system without additional components. Elasticity also provides vibration damping and an aesthetic resemblance to natural counterparts. EAPs can be divided into two major categories based on their actuation mechanisms; electric and ionic EAPs. Bar-Cohen compiled comprehensive information regarding EAP materials (Bar-Cohen, 2001).

Electric EAP

Electric EAPs induce displacement type actuation upon application of an electrical field. The actuators are composed of electrodes with an elastic polymer in between them. They possess high mechanical energy density, however, activation requires high voltage (>100V/μm). The response of the material to the electrical stimulus varies with material and this determines the subcategory of electric EAP material such as ferroelectric and electrostatic.

Ferroelectricity is a phenomenon where by dielectric materials exhibit a spontaneous electric polarization. Piezoelectric materials are a group of ferroelectric materials which release an electrical charge when stress is applied. This process is reversible so that an

applied voltage produces a material deformation. Although piezoelectricity is well known in quartz and ceramic materials, certain polymer materials such as polyvinylidene fluoride (PVDF) also possess piezoelectric characteristics. PDVF produces relatively high stress (1–4.8 MPa) at high frequency (>1000 Hz), however, the strain is limited to about 0.02% - 0.1% (Fletcher, 1996; Kornbluh et al., 1998).

Polymers with low elastic stiffness and high dielectric constant can produce large actuation strain by electrostatic attraction (Kornbluh et al., 1998; Pelrine et al., 1998). The attractive force 'squeezes' the material axially and displaces radially outward from the working axis. The unique feature of this material is the stimulation extends or relaxes the material rather than contracting it like natural muscles (Meijer et al., 2003). The material can induce a large amount of strain (60%–300%) and a relatively high stress (3-16 MPa) (Kornbluh et al., 2001). The actuators are generally composed of flexible electrodes and dielectric elastomers such as acrylic, silicone, and polyurethane.

An acrylic dielectric elastomer based EAP is one of the few active materials with which the dynamic characteristics have been examined by the work loop analysis (Full and Meijer, 2000). Stimulation (5 kV at 50% duty cycle) was applied at the cyclic phase between 270° and 90° (refer to Figure 1A, note that the material relaxes when stimulated). The highest power output of 10 W/kg was obtained at 2.5% strain with 1 Hz cyclic frequency.

Ionic EAP

Ionic EAPs utilize ionic molecular migration or diffusion for the source of actuation. The migration/diffusion of ionic molecules in the aqueous solution cause one side of the materials to 'swell'. The swelling produces a pressure gradient in the material and causes a bending motion. These materials generally require a wet environment for their operation however various approaches have been considered for dry environment operation such as the use of semi-solid electrolytes and protective coatings. Ionic EAPs generally operate at 1–10V range and have high elastic limit, however, operational frequencies and force production are relatively low. Commonly known ionic EAPs are the ionic polymer gel (IPG) (Calvert et al., 1998), ionomeric polymer-metal composite (IPMC) (Shahinpoor et al., 1998), and conductive polymer (CP) (Madden et al., 2000; Otero and Sansiñena, 1997)

IPGs such as hydrogel use an application of electric stimulation to induce an electrochemical reaction. This changes the pH level in its environment causing the material to contract or expand. Multilayered hydrogel stacks operated at 6 volts produce about 400% change in surface area in 12 minutes (Calvert et al., 1998).

IPMC utilizes the mobility of cations in the polymer network. An ion exchange polymer membrane is used as the base polymer and metal ions (i.e. platinum and gold) are deposited on the surfaces as electrodes. The operational frequency is about 0.1-35 Hz with voltage of 2-7 volts. A strip of IPMC (2cm x 4mm x 0.2mm, operated at 2 volts) produces the maximum lateral displacement (75% of total length) at the lowest frequency of 0.1Hz (Shahinpoor et al., 1998). Estimated power output of IPMC is about 10W/kg (Nemat-Nasser and Thomas, 2001).

CPs generally function by an electrochemically induced oxidation/reduction process. Typical CPs consist of a conductive polymer (i.e. polypyrrole or polyaniline) and a flexible ion-conductive polymer gel. The actuator generally requires 1-5 volt with an operational frequency of less than 1 Hz. Polyanilyne-based conductive polymer produces the maximum pressure approximately 450 MPa and a strain of about 10%.(Kornbluh et al., 2001)

Material Selection

The basic requirement for the material selection is that it is able to simulate the steady swimming of the bonito species (Table 3). The materials should have sufficient power to produce thrust, operate at least at a minimum tail beat frequency, and have an adequate strain limit to withstand bending of the body. Most materials possess reasonable mechanical properties for this application. There are significant differences in actuation mechanisms among the materials. Lack of dynamic information necessary for implementing active stretching made material selection and direct comparison between the biological and mechanical systems difficult.

Based on available information, it was decided that SMA best suit the powerful and relatively low tail beat frequencies of steady swimming. It operates at a reasonable voltage and a linear pull-type actuation mechanism closely resembles the natural muscle. Furthermore, only a few peripherals are required for its operations and the materials are readily available. The moderate amount of strain limit poses some concerns, however, this can be improved by geometric arrangement.

Nickel-Titanium based SMA wire was selected for the actuator material. The actuators are controlled by pulse width modulated signals (PWM) from a microprocessor. Position information from sensors is used to control firing sequence and simulating active stretching of each actuator. The firing sequence of each actuator along the body is based on red muscle stimulation pattern of bonito (*Sarda Chiliensis*) (Ellerby et al., 2000). Prior to defining the control sequence, the dynamic properties of SMA will be examined using work loop analysis. This information will be used to adjust stimulation timing and duration to optimize the system operation.

Design considerations using SMA

Important design factors to be considered for the application of SMA wires are the thermal management and the strain limitation. Quick removal of the heat from the wire improves the relaxation time. Incorporating heat sink mediums such as water and heat transfer fluids could improve the operational frequency. A current regulated PWM driver reduces the chance of overheating and provides efficient power delivery. Minimizing the wire diameter could also improve cyclic frequency.

Maintaining the actuation range within its strain limit is important for longer operational life. Placing the actuators along the lateral line (away from neutral axis) increases the mechanical leverage for bending a body but this may cause the wire to exceed its strain limit. Spring-formed SMA wires could alleviate the problem, however, this significantly reduces the force output.

Oblique arrangements are an alternate method that can be used in order to gain a mechanical advantage by trading force for distance (Gilbertson, 2000). The following figures show the effect on oblique arrangement of a SMA wire. Simple geometrical analysis indicates that reducing the triangle height or the wire angle increases the actuation ranges while decreasing the resulting forces.

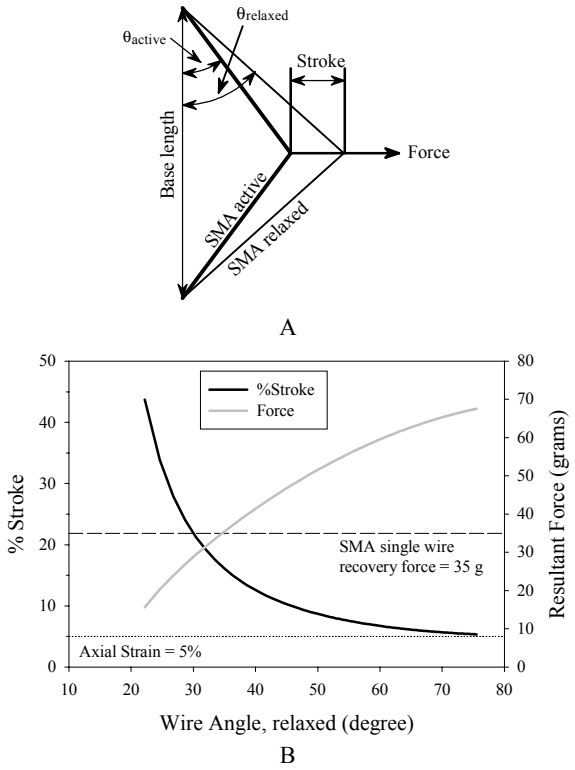

Figure 4. Oblique Wire Arrangement. A. schematic representation of oblique arrangement adapted from *(Gilbertson, 2000)*. B. plot of oblique angle vs. resultant stroke and force production. (diameter = 50μm, applied strain = 5%, recovery force = 35g).

Design of propulsive mechanism

The oscillating propulsion system is based on a segmented actuator system, the arrangements of the actual superficial red muscle and on the connective tissues (Figure 5). The backbone is made of a flexible sheet and segmented actuator units are attached to it. SMA wires are attached to the ends of laterally extending columns, arranged in backward pointing 'V' shape across two segments. Tendon-like high modulus and low extension materials are extending across a few segments. A head cavity and a portion of the ventral or bottom region is used to store electronic components and the rest of body cavity will be filled with a low viscosity dielectric gel and covered with an elastic fabric to maintain body shape.

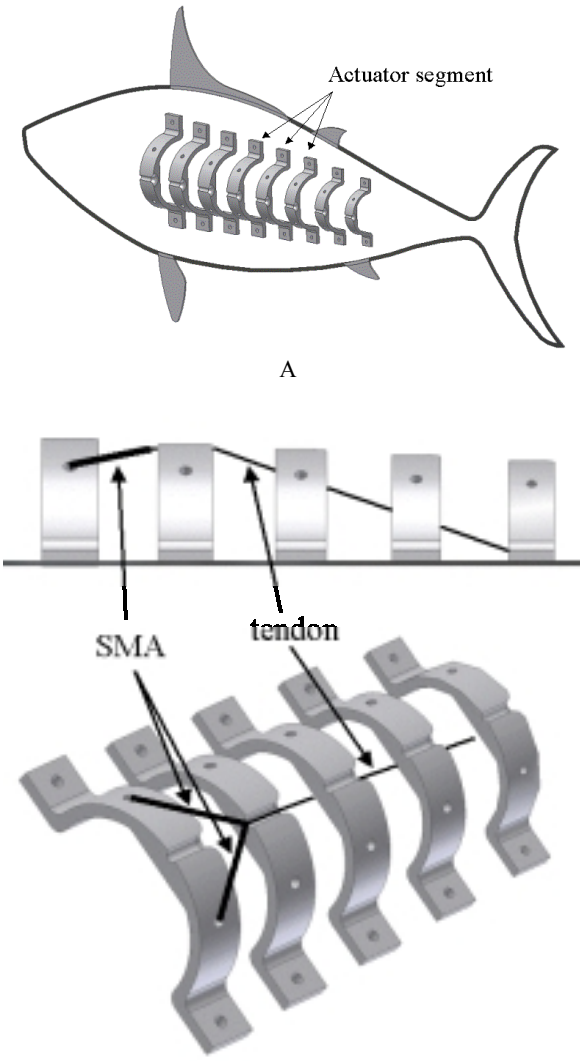

Figure 5. Schematic design of an oscillating propulsive mechanism. A. general view B. detailed arrangement of a SMA wire and tendon.

Several wire arrangements were examined for estimating the force production and range of motion. Samples of Atlantic bonitos (*Sarda sarda*) were obtained for morphological measurements. Based on the samples, the geometrical arrangement of the tendons and the force productions were examined at three locations from snout with respect to a body length, BL (Table 4). The tendon angles and muscle strain at each body position were taken from Table 2 and Table 3 respectively.

Table 4. Tendon geometry and force production.

Body Length, BL	49.5 cm		
Fork Length, FL	45.7 cm		
Position	0.35 BL	0.5BL	0.65 BL
Biological Information			
AOT angle	50°	65°	80°
POT angle	40°	25°	10°
Muscle strain	±3.1%	±5.2%	±5.8%
% red muscle area	7.5 %	15 %	25 %
Morphological information of a model			
AOT length	4.8 cm	3.4 cm	2.1 cm
POT length	5.7 cm	7.3 cm	11.9 cm
Base length	7.4 cm	8.1 cm	12.1 cm
Section width	7.3 cm	6.2 cm	4.1 cm
Red muscle area	4.9 cm^2	7.8 cm^2	6.3 cm^2
Calculated parameters			
Velocity ratio	1.56	2.37	5.76
Section force	34.4 N	54.4 N	44.1 N
Lateral force	22.1 N	23.0 N	7.7 N
Tendon span over the vertebra	6	7	9
Force transmission per tendon	5.7 N	7.8 N	4.9 N

The AOT, POT and base lengths were obtained by simple geometrical calculations. A hypothetical muscle length of 7.5cm (Westneat and Wainwright, 2001) was used to obtain the amount of muscle shortening at each position. Since the POT slid over the sling, the muscle shortening directly translated into the shortening of the POT length (Figure 3B). Assuming the AOT, base length, and the body width, remain constant, the lateral deflection at the end of POT and the velocity ratio were calculated. The velocity ratio indicates the mechanical leverage obtained by this arrangement and is expressed as the ratio of the lateral displacement to muscle displacement.

The amount of red muscle at each body position was estimated by using the red muscle distribution of pacific bonito (Ellerby et al., 2000). The muscle forces were then calculated assuming 140kN/m^2 was the nominal stress production (Table 1) and only a half of the red muscle area was active at a time.

These calculations indicate that the primary force production occurred at the anterior section while the posterior section contributed to the lateral displacement. The POT length doubled at the posterior which indicates the tendons span more vertebra joints than the anterior section. The length of each vertebra segment of the model between 0.3BL and 0.65BL was approximately 1.3mm. Therefore the spans of the tendons over the vertebra were 6, 7, and 9 vertebras at 0.35BL, 0.5BL, and

0.65BL respectively. This closely matched with the estimated tendon spans of tuna (*Euthynnus alletteratus*) (Westneat and Wainwright, 2001). This also indicated that several of the tendons overlap each other, increasing the force output at a given cross section and allowing smooth lateral displacement transitions from one joint to the other. The force transmitted by each POT tendon was approximately 5-8 N. This was estimated by dividing the total force produced at each position by the number of overlaps.

From Figure 4B, a 50μm SMA wire at $\theta_{relaxed} = 30°$ produces about 0.3N. It requires 17-27 bundles to produce 5-8 N at each segment. The amount of stroke obtained with this arrangement was 15% which satisfied the maximum strain requirement in bonito swimming (Table 3).

Concluding Remarks

The process of developing a biologically inspired system requires that the differences in the design strategies between the biological and mechanical components be recognized. A blind copy of nature is likely to fail due to the complexity in biological systems (Vogel, 1998). Evolution has adapted a 'just good enough' approach to component design; they may not excel at a particular task but perform many functions sufficiently (Meijer et al., 2003). Mechanical components, on the other hand, have particular advantages for certain types of activities (Full and Meijer, 2000). The successful adaptation of a biological system is to identify/extract the key principles of the activity and evaluate/design the mechanical system accordingly (Full and Meijer, 2001; Meijer et al., 2003).

The use of elastic systems in the scombrid propulsion system was investigated. The data suggested that the application of active stretching could improve the efficiency and power output of mechanical systems. However, the dynamic properties necessary for adapting such a scheme are not available in many engineering materials. Work loop technique to describe the dynamic properties of an electrostatic EAP was demonstrated (Full and Meijer, 2000) and this can be adapted to other engineering materials.

SMAs and EAPs were examined as potential actuator materials for implementing the steady swimming of the bonito species. Specifying the particular mode of muscle activity was necessary due to the limited capability of engineering materials. Differences in actuation mechanisms were found and this made any direct comparison among the materials difficult. Virtually any material can by used to simulate a specific mode of muscle activity, however, SMA was best suited to the steady swimming which involves powerful and low frequency muscle activities. The limited range of motion in SMA was enhanced by the triangular wire arrangement. Oblique tendon arrangements in scombrid species were also utilized to provide force transmission pathways to the backbone and to gain mechanical advantages in order to bend the body.

The muscle stimulation sequence along the body and stimulation timing with respect to the strain cycle are available. This information can be utilized to implement an active stretching effect in SMA. The dynamic response of SMA under such conditions is not known and will be investigated by adapting a work-loop technique.

Acknowledgment

The author would like to acknowledge the support of the Link Foundation.

References

Alexander, R. M. (1969). The orientation of muscle fibers in the myomere of fishes. *J. mar. biol. Ass. U.K.* **49**, 263-390.

Alexander, R. M. (1984). Elastic energy stores in running vertebrates. *Amer. Zool.* **24**, 85-94.

Alexander, R. M. (1988). Elastic mechanisms in animal movement. Cambridge, UK: Cambridge University Press.

Altringham, J. D. and Ellerby, D. J. (1999). Fish swimming: patterns in muscle function. *J. exp. Biol.* **202**, 3397-3403.

Altringham, J. D. and Johnston, I. A. (1990). Scaling effects in muscle function: power output of isolated muscle fibers performing oscillatory work. *J. exp. Biol.* **151**, 453-467.

Altringham, J. D. and Shadwick, R. E. (2001). Swimming and muscle function. In *Tuna: physiology, ecology, and evolution*, eds B. A. Block and E. D. Stevens), pp. 313-344. San Diego: Academic Press.

Ayers, J., Wilbur, C. and Olocott, C. (2000). Lamprey Robots. In *Proc. Int'l Symp. Aqua Biomechanisms*, eds. T. Wu and N. Kato). Tokai University.

Bandyopadhay, P. R. (1998). Phase vortex seeding for thrust modulation in a rigid cylinder with flapping foil thrusters. In *Proc. Int'l Symp. Sea Water Drag Reduction*, pp. 457-469. Newport, RI.

Bar-Cohen, Y. (2001). Electroactive polymer (EAP) actuators as artificial muscles - reality, potential, and challenges. Bellingham, WA, USA: SPIE Press.

Bennett, M. B., Ker, R. F. and Alexander, R. M. (1987). Elastic properties of Structures in the tails of cetaceans (*Phocaena* and *Largenorhynchus*) and their effect on the energy cost of swimming. *J. Zool., Lond.* **211**, 117-192.

Biewener, A. A. (1998). Muscle function *in vivo*: a comparison of muscles used for elastic energy savings versus muscles used to generate mechanical power. *Amer. Zool.* **38**, 703-717.

Blickhan, R. and Cheng, J.-Y. (1994). Energy storage by elastic mechanisms in the tail of large swimmers - a re-evaluation. *J. theor. Biol.* **168**, 315-321.

Breazeal, C. and Bar-Cohen, Y. (2003). Introduction to biomimetic inteligent robots. In *Biologically inspired intelignet robot*, eds Y. Bar-Cohen and C. Breazeal), pp. 1-24. Bellingham, WA: SPIE press.

Calvert, P., O'kelly, J. and Souvigner, C. (1998). Solid freeform fablication of organic-inorganic hybrid materials. *Mat. Sci. and Eng.* **C 6**, 167-174.

Carlson, F. D. and Wilkie, D. R. (1974). Muscle physiology. Englewood, NJ: Prentice-Hall.

Ellerby, D. J., Altringham, J. D., Williams, T. and Block, B. A. (2000). Slow Muscle Function of Pacific Bonito (Sarda Chiliensis) during steady swimming. *J. exp. Biol.* **203**, 2001-2013.

Farley, C. T., Glasheen, J. and McMahon, T. A. (1993). Running springs: speed and animal size. *J. exp. Biol* **185**, 71-86.

Fish, F. E. and Rohr, J. J. (1998). Review of Dolphin Hydrodynamics and Swimming Performance (TR1801). San Diego, C.A.: Space and Naval Warfare Systems Command.

Fletcher, R. (1996). Force transduction materials for human-technology interfaces. *IBM Systems Journal* **35**, 630-638.

Full, R. J. (1997). Invertebrate locomotor systems. In *The handbook of Comparative Physiology*, (ed. W. Dantzler), pp. 853-930. Oxford, U.K.: Oxford University Press.

Full, R. J. and Meijer, K. (2000). Artificial muscles versus natural actuators from frog to flies. *Proceedings of the SPIE* **3987**, 2-9.

Full, R. J. and Meijer, K. (2001). Metrics of natural muscle functions. In *Electroactive polymer (EAP) actuator as artificial muscles - reality, potential, and challenges*, (ed. Y. Bar-Cohen), pp. 67-81. Bellingham, WA, USA: SPIE press.

Gilbertson, R. G. (2000). Muscle wires project book. San Rafael, CA, USA: Mondo-tronics, Inc.

Hodgson, D. E. (1988). Using Shape Memory Alloys. Sunnyvale, CA: Shape Memory Applications, Inc.

Hollerbach, J. M., Hunter, I. W. and Ballantyne, J. (1992). A comparative Analysis of Actuator Technologies for Robotics. In *The Robotics Review 2*, eds O. Khatib J. J. Craig and T. Lozano-Pérez), pp. 299-342. Cambridge, M.A.: MIT Press.

Jackson, C. M., Wagner, H. J. and Wasilewski, R. J. (1972). 55-Nitinol - The Alloy with a Memory: Its Physical Metallurgy, Properties, and Applications. Washington D.C.: NASA.

Josephson, R. K. (1985). Mechanical power output from striated muscle during cyclical contraction. *J. exp. Biol.* **114**, 493-512.

Ker, R. F. (1981). Dynamic tensile properties of the plantaris tendon of sheep (*Ovis aries*). *J. exp. Biol.* **93**, 283-302.

Knower, T., Shadwick, R. E., Katz, S. L., Graham, J. B. and Wardle, C. S. (1999). Red Muscle activation pattern in yellowfin (*Thunnus albacores*) and skipjack (*Katsuwonus pelamis*) tunas during steady swimming. *J. exp. Biol.* **202**, 2127-2138.

Kornbluh, R., Pelrine, R., Eckerle, J. and Joseph, J. (1998). Electrostrictive polymer artificial muscle actuator. In *Proc. IEEE Int. conf. Robotics and Automation (ICRA '98)*, pp. 2147-2154. Leuven, Belgium.

Kornbluh, R., Pelrine, R., Pei, Q. and Shastri, S. V. (2001). Application of dielctric elastomer EAP actuator. In *Elactroactive Polymer (EAP) actuators as artificial muscles - reality, potential, and challenges*, (ed. Y. Bar-Cohen), pp. 457-495.

Lindstedt, S. L., Reich, T. E., Keim, P. and LaStayo, P. C. (2002). Review: do muscle function as adaptable locomotor springs? *J. exp. Biol.* **205**, 2211-2216.

Madden, J. D., Cush, R. A., Kanigan, T. S. and Hunter, I. W. (2000). Fast contracting polypyrrole actuators. *Synthetic Mat.* **113**, 185-192.

McMahon, T. A. (1984). Muscles, reflexes, and locomotion. Princeton, N.J.: Princeton University Press.

Meijer, K., Bar-Cohen, Y. and Full, R. J. (2003). Biological inspiration for musclelike actuators on robot. In *Biologically inspired intelligent robot*, eds Y. Bar-Cohen and C. Breazeal). Bellingham, WA, USA: SPIE Press.

Nachtigall, W. (1974). Insects in flight; a glimpse behind the scenes in biophysiological research. New York: McGraw-Hill.

Nemat-Nasser, S. and Thomas, C. W. (2001). Ionomeric polymer-metal composites. In *Electroactive polymer (EAP) actuators as artificial muscles - reality, potential, and challenges*, (ed. Y. Bar-Cohen), pp. 139-191. Bellingham, WA: SPIE Press.

Nordin, M. and Frankel, V. H. (2001). Basic biomechanics of the musculoskeletal system. Baltimore, MD: Lippincott Williams & Wilkins.

Nursall, J. R. (1956). The lateral musculature and the swimming if fish. *Proc. Zool. Soc., Lond.* **126**, 127-143.

Otero, T. F. and Sansiñena, J. M. (1997). Bilayer dimensions and movement in artificial muscles. *Bioelectrochemistry and Bioenergetics* **42**, 117-122.

Pelrine, R. E., Kornbluh, R. D. and Joseph, J. P. (1998). Electrostriction of polymer dielectrics with compliant electrodes as a means of actuation. *Sensors Actuat. A* **64**, 77-85.

Rome, L. C. (1994). The mechanical design of the fish muscular system. In *Mechanics and physiology of animal swimming*, eds L. Maddock Q. Bone and J. M. V. Rayner), pp. 75-97. New York: Cambridge University Press.

Sfakiotakis, M., Lane, D. M. and Davies, B. C. (1999). Review of fish swimming modes for aquatic locomotion. *IEEE J. Oceanic Eng.* **24**, 237-252.

Shadwick, R. E., Katz, S. L., Korsmeyer, K. E., Knower, T. and Covell, J. W. (1999). Muscle dynamics in skipjack tuna: Timing of red muscle shortening in relation to activation and body curvature during steady swimming. *J. exp. Biol.* **202**, 2139-2150.

Shahinpoor, M., Bar-Cohen, Y., Simpson, J. O. and Smith, J. (1998). Ionic polymer-metal composites (IPMC) as biomimetic sensors, actuators and artificial muscles - a review. *Smart Marter. Struct.* **7**, R15-R30.

Syme, D. A. and Shadwick, R. E. (2002). Effects of longitudinal body position and swimming speed on mechanical power of deep red muscle from skipjack tuna (Katsuwonus pelamis). *J. exp. Biol* **205**.

Triantafyllou, M. S. and Triantafyllou, G. S. (1995). An Efficient Swimming Machine. *Sci. Am.* **272**, 63-70.

Van Leeuwen, J. L. (1999). A mechanical analysis of myomere shape in fish. *J. exp. Biol.* **202**, 3450-3414.

Vogel, S. (1998). Cat's paws and catapults. New York: Norton.

Wainwright, S. A. (1983). To bend a fish. In *Fish Biomechanics*, eds P. W. Webb and D. Weihs), pp. 68-91. New York: Praeger Publishers.

Webb, G., Wilson, L., Lagoudas, D. and Rediniotis, O. (2000). Adaptive control of shape memory alloy actuators for underwater biomimetic applications. *AIAA Journal* **38**, 325-334.

Westneat, M. W. and Wainwright, S. A. (2001). Mechanical design for swimming: muscle, tendon, and bone. In *Tuna: physiology, ecology, and evolution*, vol. 19 eds B. A. Block and E. D. Stevens), pp. 271-311. San Diego: Academic Press.

White, D. C. S. (1977). Muscle mechanics. In *Mechanics and energetics of animal locomotion*, eds R. M. Alexander and G. Goldspink), pp. 23-56. N.Y.: Cambridge University Press.